FERMILAB-PUB-08-244-ESH-REV
To be published in *Health Physics*

NEUTRON DOSE PER FLUENCE AND WEIGHTING FACTORS FOR USE AT HIGH ENERGY ACCELERATORS

J. Donald Cossairt and Kamran Vaziri*
Revised December 2008

ABSTRACT

In June 2007, the United States Department of Energy incorporated revised values of neutron weighting factors into its occupational radiation protection regulation Title 10, Code of Federal Regulations Part 835 as part of updating its radiation dosimetry system. This has led to a reassessment of neutron radiation fields at high energy accelerators such as those at the Fermi National Accelerator Laboratory (Fermilab) in the context of the amended regulation and contemporary guidance of the International Commission on Radiological Protection. Values of dose per fluence factors appropriate for accelerator radiation fields calculated elsewhere are collated and radiation weighting factors compared. The results of this revision to the dosimetric system are applied to americium-beryllium neutron energy spectra commonly used for instrument calibrations. Also, a set of typical accelerator neutron energy spectra previously measured at Fermilab are reassessed in light of the new dosimetry system. The implications of this revision and of recent ICRP publications are found to be of moderate significance.

Key words: accelerators, neutron dosimetry, instrumentation, quality factor

INTRODUCTION

For all facilities, including particle accelerators, regulated by the United States Department of Energy (DOE), occupational radiation protection requirements are set forth in Title 10, Code of Federal Regulations Part 835 (10 CFR Part 835), *Occupational Radiation Protection*. In June 2007, amendments to this regulation were finalized (U. S. DOE 2007). Undoubtedly the most significant change was the incorporation of the system of dosimetry instituted by the International Commission on Radiological Protection (ICRP) in its Publications 60 (ICRP 1990) and 68 (ICRP 1994). ICRP Publication 68 solely deals with internal exposure, only rarely encountered at accelerators, and is not applicable to the topic of this paper. ICRP Publication 60 has since been updated further by the ICRP in Publication 74 (ICRP 1996) and most recently in Publication 103 (ICRP 2007). DOE facilities are required to be in full compliance with the amended regulation by 9 July 2010. 10 CFR Part 835 is limited in its applicability to occupational settings; DOE addresses radiation protection of the public and environment separately in DOE Order 5400.5 (U. S. DOE 1993). This Order incorporates the dosimetry system now superseded by the amended 10 CFR Part 835. It is anticipated that DOE Order 5400.5 will be revised to match the dosimetry system of the amended regulation to remove this ambiguity.

To implement the new requirements, it is necessary to understand the new radiation dosimetry system, apply it to radiological conditions present at accelerators, and implement changes in calibrations and practices found to be necessary. At particle accelerators, the predominant impact of the regulatory amendments applies to the neutron-dominated external radiation fields. While considerable investments in design and in civil construction have resulted in most prompt radiation fields at accelerators being shielded to levels near or below natural background in locations accessible to people, nearly all accelerators have a few accessible locations where measurable neutron-dominated radiation fields can be found in addition to the intense radiation fields found in areas inside accelerator enclosures that are inaccessible during operations.

RADIOLOGICAL QUANTITIES

Prior to the amendments of 2007, 10 CFR Part 835 addressed neutron radiation fields using a dimensionless quality factor, Q_{H}, as the connection between the physical quantity absorbed dose, D (Gy), and the radiation protection quantity dose equivalent, H (Sv);

$$H = Q_{\mathrm{H}} D \,, \quad (1)$$

consistent with recommendations of the ICRP and the National Council on Radiation Protection and Measurements (NCRP) predating ICRP Publication 60[†]. For selected neutron kinetic energies, T_{n}, the pre-2007 versions of 10 CFR Part 835 provided tabular values of Q_{H} and P_{H}, the dose equivalent per fluence. The values were taken from NCRP Report 38 (NCRP 1971) and are consistent with those of ICRP Publication 26 (ICRP 1981). These are given in Table 1, with suitable unit conversions made for consistency with other references[‡]. Perhaps surprisingly, 10 CFR Part 835 as amended in 2007 does not provide any explicit values of a replacement for P_{H} connecting fluence to dosimetric quantities.

The documents describing the new dosimetry system introduce a number of radiological quantities. Descriptions of several of these quantities adapted for present purposes from those of ICRP Publication 74 (ICRP 1996) and the amended 10 CFR 835 (DOE 2007) are given below:

Absorbed dose, D (J kg^{-1}, special unit Gy), is the mean energy imparted by ionizing radiation to a unit mass of matter. It is, in principle, a quantity that is physically measurable.

Ambient dose equivalent, $H^*(d)$ kg^{-1}, special unit Sv), is the dose equivalent, measured at each point in a radiation field that would be produced in the corresponding expanded and aligned field in the ICRU sphere[§] at depth, d, on the radius opposing the direction of the aligned field.

Equivalent dose, $H_{T,R}$ (J kg^{-1}, special unit Sv), is the absorbed dose in an organ or tissue multiplied by the relevant radiation weighting factor, w_R.

Effective dose, E (J kg^{-1}, special unit Sv), is the summation of equivalent doses in tissues or organs each multiplied by the appropriate organ weighting factors specified in the ICRP Publications cited. E is also the sum of all absorbed doses weighted by radiation weighting factors and by the correct organ weighting factors of the entire body.

Personal dose equivalent, $H_p(d)$ (J kg^{-1}, special unit Sv), is the equivalent dose in soft tissue defined at depth, d, below a specified point in the body.

Operational quantities such as $H^*(d)$ and $H_p(d)$ are measurable, at least in principle, and can be used to determine the properties of radiation fields to estimate and demonstrate compliance with specified standards.

Protection quantities such as E and $H_{T,R}$ are used to determine conformance with numerical limits and action levels in radiation protection standards. They are theoretical and not measurable.

Radiation weighting factor, w_R, is the factor by which the tissue or organ absorbed dose is multiplied to reflect relative biological effectiveness (RBE) values. For external radiation fields, it supersedes Q_H and, like Q_H, is dimensionless. References cited, e.g. ICRP Publication 74 (ICRP 1996), endorse the ongoing validity of the concept of an average quality factor, $\langle Q \rangle$.

The revised 10 CFR Part 835 invokes E as a protection quantity and connects this with the operational quantity $H_p(d)$ measured or calculated at specified depths, d, for various tissues. For the lens of the eye, skin and extremities, and the whole body, d is to be taken to be 3 mm, 0.07 mm, and 10 mm, respectively. Since the scope of this paper is limited to whole body external radiation fields, d = 10 mm is implicit. $H_p(10\ mm)$ is the operational quantity recommended for demonstrating compliance with the annual limits, etc. for such radiation fields. Without the need to consider internal exposures, it can be taken as equivalent to E for the whole body and implicitly incorporates the appropriate tissue weighting factors specified by the recent ICRP Publications.

DOSE PER FLUENCE CONVERSION FOR NEUTRONS

To understand the response of instrumentation and interpret shielding calculations, one needs to connect the neutron fluence**, Φ (cm^{-2}), with a dosimetric quantity such as E. However, the amended 10 CFR Part 835 does not continue to provide a table of values of P_E, the effective dose per fluence;

$$P_E = E\ \Phi^{-1}. \quad (2)$$

At accelerators these factors can be needed for the energy domain from "thermal" up to essentially the beam energy. The use of the dosimetry quantities requires a selection of exposure geometry from standardized models. These models assume that the orientation of the exposed person relative to the neutron source is known, a condition likely unrealistic in a typical workplace or environmental setting. Two of the models, called ROT and ISO, appear to best match workplace conditions at accelerators. ROT geometry is defined in ICRP Publication 74 (ICRP 1996) to be that where the body is irradiated by a parallel beam of ionizing radiation from a direction orthogonal to the long axis of the body rotating at a uniform rate about its long axis. While this "shish kebab" picture is preferable to the alternatives that involve a static orientation, it is clearly imperfect. In ISO (isotropic) geometry, also imperfect, the fluence per unit solid angle is independent of direction (ICRP 1996). ROT is preferred and used when possible here.

Fig. 1 shows various dose per fluence values as a function of neutron kinetic energy, T_n, including those for dose equivalent H. For ease of reading, Fig. 1 has been divided into three energy domains. ICRP Publication 74 (ICRP 1996) provides values for P_E for 10^{-9} MeV $\leq T_n \leq$ 180 MeV for ROT geometry. Sutton-Ferenci et al. (2000) have calculated P_E for ROT geometry up to T_n = 2 GeV. Guided by Harvey and Mill (1985), they use a formula that describes their own results and the ICRP Publication 74 values for 10^{-9} MeV $\leq T_n \leq$ 2000 MeV;

$$\log_{10}\{P_E(T_n)\} = \frac{a}{1+(b+c\log_{10}T_n)^2} + \frac{d}{1+\exp(f-g\log_{10}T_n)} + \frac{h}{1+\exp(j-k\log_{10}T_n)}. \quad (3)$$

For ROT geometry Table 2 gives the parameters *a, b, c, d, f, g, h, j,* and *k*. Fig. 1 also includes P_p and P^*, denoting $H_p(10\text{ mm})\Phi^{-1}$ and $H^*(10\text{ mm})\Phi^{-1}$, respectively, calculated by Veinot and Hertel (2005) for 10^{-9} MeV $\leq T_n \leq$ 20 MeV. In surveying these results, it is clear that the value of P_H is actually smaller than that of P_E over rather large domains of T_n. The proper values should be incorporated into Monte Carlo shielding calculations to enable efficient shielding design.

At accelerators, conversion factors for even higher energy neutrons can be needed. Fig. 1 thus includes the values of P_E calculated by Ferrari et al. (1997) for ISO geometry for 2.5 x 10^{-8} MeV $\leq T_n \leq 10^7$ MeV as well as those of P^* calculated by Stevenson (1986) for 2.5 x 10^{-8} MeV $\leq T_n \leq$ 9 x 10^6 MeV. From Fig. 1 it is evident that the dose per fluence increases considerably in the multi-GeV regime, consistent with intuition connected with the rapid increase of secondary particle multiplicity with increasing hadronic energies (e.g., Particle Data Group 2006). As expected this increase is not reflected by Eq. (3) above the domain of its fitting. From the nature of the interactions of high energy neutrons with matter it is sensible that in this energy regime P_E and P^* track together. Given the overall consistency of the results of Ferrari et al. with the other

dosimetric quantities in terms of general energy dependence and overall magnitudes, an adjunct to Eq. (3) in the form of power law fit is found for $T_n > 2000$ MeV, with T_n in MeV, and shown in Fig. 1;

$$P_E = mT_n^p \text{ (pSv cm}^2\text{)}. \quad (4)$$

The values of m and p determined by a least squares fit are given in Table 2. Eq. (4) fits the referenced calculations well over this energy domain. Eqns. (3) and (4) describe the energy dependence of P_E over the domain found at particle accelerators and were used to calculate the values listed in Table 3. Eqns. (3) and (4) are offered as a tool for use in practical work, they are not fundamental calculations of dose per fluence.

RADIATION WEIGHTING FACTORS

One also needs values of quality factor, Q, or radiation weighting factor, w_R, to connect absorbed dose to a radiation-weighted quantity in the model of Eq. (1). Fig. 2 shows various weighting factors. Included are values of neutron quality factor from NCRP Report 38 (NCRP 1971), Q_H; the essentially identical weighting factors given in ICRP Publication 60 (ICRP 1990) and 74 (ICRP 1996); and the most recent values of ICRP Publication 103 (ICRP 2007). Fig. 2 also includes the quality factors Q_p and Q^* connected with $H_p(10\text{ mm})$ and $H^*(10\text{ mm})$ calculated by Veinot and Hertel (2005) and the values of Q_E of Ferrari and Pelliccioni (1998) connected with E. The latter cover a particularly large energy domain. In contrast with the situation observed for P_E in comparison with P_H, except for some of the domain $10 < T_n < 100$ MeV, the value of the weighting or effective quality factors using the newer ICRP publications is nearly always larger than Q_H.

Formulae to describe these weighting factors are recommended. For T_n in MeV ICRP Publication 60 gives:

$$w_{R,60}(T_n) = 5.0 + 17.0\exp\left[-\{\ln(2T_n)\}^2/6\right]. \quad (5)$$

For T_n in MeV ICRP Publication 103 has updated this recommendation to:

$$w_{R,103}(T_n) = 2.5 + 18.2\exp\left[-\{\ln(T_n)\}^2/6\right], \quad T_n < 1 \text{ MeV} \quad (6)$$

$$w_{R,103}(T_n) = 5.0 + 17.0\exp\left[-\{\ln(2T_n)\}^2/6\right], \quad 1 \text{ MeV} \le T_n \le 50 \text{ MeV} \quad (7)$$

$$w_{R,103}(T_n) = 2.5 + 3.25\exp\left[-\{\ln(0.04T_n)\}^2/6\right], \quad T_n > 50 \text{ MeV}. \quad (8)$$

Table 4 gives values of w_R calculated according to Eqns. (5)-(8). Eqns. (5) - (8) are offered as a tool for use in practical work, they are not fundamental calculations of the radiation weighting factor.

APPLICATION TO AMERICIUM-BERYLLIUM NEUTRON SPECTRA

Alpha-neutron sealed sources including ^{241}Am-Be provide neutron radiation fields used for instrument calibrations at many institutes, including Fermilab. It is prudent to reassess the radiation fields produced by these sources to correctly understand the instrument response. For example, at Fermilab, the most prominent neutron-sensitive instruments are the "chipmunk" ion chambers (Krueger and Larson 2002).

There is a plethora of published ^{241}Am-Be neutron spectra. These spectra are rather difficult to measure since the domain of energy involved is that where instrument responses, including energy thresholds and strongly energy-dependent efficiencies, have to be untangled. Also, details of construction of these sources; including the physical dimensions, geometric configuration, and encapsulation materials; can affect the spectrum. The geometry of the irradiation exemplified prominently by the presence or absence of concrete walls will also influence the results. Since the calibration facility at Fermilab lacks the instrumentation needed to directly measure the ^{241}Am-Be energy spectrum to high resolution, published results were used. Fig. 3 displays the International Standards Organization ISO 8529-1 spectra (ISO 2001) extracted graphically from the paper of Zimbal (2007) as well as the spectrum calculated by DeGuarrini and Malaroda (1971).

Fluence-weighted average energies, mean neutron radiation weighting factors, and mean dose per fluence factors were determined for these neutron spectra and given in Table 5. This was done by numerically integrating over energy bins of 0.1 MeV. The uncertainty of the results is dominated by the details of source construction and of the irradiation conditions, not by this choice of bin size. The number of neutrons in each bin was taken from the tabulated spectra and multiplied by the values of P_E calculated with Eqns. (3) and (4) to determine E for that bin. The w_R values calculated using Eq. (5) [ICRP Publications 60 and 74] and Eqns. (6)-(8) [ICRP Publication 103] were used to extract the absorbed dose, D, due to that bin. Similarly, H was determined from the fluence spectra and interpolations of the values in Table 1. After numerically integrating to get E, H, and D for the entire energy spectra, the average effective quality factors, $\langle Q_E \rangle_{60}$ and $\langle Q_E \rangle_{103}$ were deduced and compared with $\langle Q_H \rangle$ determined from H. No difference between the results for $\langle Q_E \rangle$ obtained using each of the newer ICRP publications (ICRP 1990; ICRP 1996; ICRP 2007) is evident, as expected for the energy domain of the neutrons spectra emitted by the ^{241}Am-Be sources. Numerical integrations were similarly performed to determine average values of $\langle P_E \rangle_{103}$ and $\langle P_H \rangle$ and their ratios for these spectra. $\langle P_E \rangle_{103}$ does not differ significantly from $\langle P_E \rangle_{60}$ for these spectra. Notably, these results take into account only the neutrons emitted by the source; secondary radiations generated by the source such as photons, neutrons scattered by room walls and the floor or ground, or thermalized neutrons are ignored. These additional radiations that likely reduce the quality factor of the complete radiation field may be important in practical work. The cumulative contributions to neutron energy spectra are useful. Fig. 4 shows these distributions for E, D, and H.

The new results should be used to revise the calibrations of neutron-sensitive instruments employed to measure properties of the radiation field. For example, the recombination chamber technique (Sullivan and Baarli 1963) is used to perform such measurements at Fermilab (Cossairt et al. 1985; Elwyn and Cossairt 1986; Cossairt and Elwyn 1987). In view of the change

to the new dosimetry system, the calibration of such an instrument should be modified to incorporate the new values.

APPLICATION TO ACCELERATOR NEUTRON ENERGY SPECTRA

To further understand the impact of the new neutron weighting factors, they were applied to neutron radiation fields previously characterized at Fermilab representative of the diversity of beam and shielding configurations present. Denoted A-I, the spectra were measured using the Bonner sphere technique (Bramblett et al. 1960) as described in detail elsewhere (e.g., Cossairt et al. 1988). Figs. 5-7 show both the configuration involved and the measured neutron energy spectra in arbitrary units of neutrons per logarithmic energy interval, $N(T_n)/\Delta\log_{10}(T_n)$, quaintly called "lethargy" plots. To detect the thermalized neutrons, the exothermic $^6Li(n,\alpha)^3H$ thermal neutron capture reaction (nuclear reaction Q-value = 4.78 MeV) was used. For eight of the spectra, a $^6Li(Eu)$ crystal embedded in plastic scintillator as a so-called "phoswich" detector was used to provide an active (e.g. "live") readout, preferred because of its background subtraction capability (Awschalom and Coulson 1973). The responses of the spheres were measured one at a time to avoid confounding the data with radiation field non-uniformities and sphere-to-sphere thermalization (i.e.,"cross-talk").

Spectrum A arose from the targeting of protons having a kinetic energy of 8 GeV on a magnet in the Fermilab Debuncher storage ring. This storage ring is normally used to store 8 GeV antiprotons. The spheres were located external to a 671 g cm^{-2} shield of earth and ordinary concrete. The earth shield was of high density ($\rho \approx 2.25$ g cm^{-3}) glacial till soil sandwiched between the concrete roof of the storage ring enclosure and the concrete floor of the building where the measurement was made with the spheres. Each layer of concrete ($\rho \approx 2.4$ g cm^{-3}) was about 30 cm thick.

Spectrum B resulted from the targeting of 8 GeV protons on a magnet in a different location in the same Fermilab Debuncher storage ring where spectrum A was measured. Here the spheres were placed external to a 402 g cm^{-2} thick shield of earth and concrete capped with a slab of iron approximately 30 cm thick. The spheres rested on an iron grating above the iron slab.

Spectrum C was obtained inside of the enclosure of the superconducting Tevatron proton synchrotron. At the time of the measurement the "warm iron" (i.e., non-superconducting) 150 GeV Main Ring proton synchrotron was also located in this tunnel and served as the injector to the Tevatron. The Bonner spheres were located near the opposite wall as shown. The neutrons were produced from 800 GeV protons interacting with a controlled low-pressure stream of nitrogen gas introduced into the Tevatron vacuum chamber during circulating beam conditions with protons of no other energies present in the enclosure (McCaslin et al. 1988).

Spectrum D was obtained relatively far downstream of a large target and beam absorber struck by 800 GeV protons and shielded by iron and concrete located in the P-Center beamline of the Fermilab fixed-target experimental areas (Cossairt and Elwyn 1987).

Spectra E and F were obtained lateral to a large electromagnet (≈ 15 m long) that contained beam absorbers within its gap. The magnet served as a large aperture magnetic spectrometer for the

secondary charged particles, principally muons, intrinsic to the high-energy physics experiment downstream of the region shown in the Fig. 6. Here 800 GeV protons interacted with a production target and, along with many of the secondary hadrons, were removed in a beam absorber at the upstream end of the magnet (not shown). However, a significant intensity of secondary hadrons of multi-hundred GeV energies struck the secondary particle absorber comprised of lead bricks shown in Fig. 6. Spectrum E was measured with the spheres viewing the bare iron of the magnetic field return yoke of the magnet while spectrum F was measured with the magnetic field return yoke partially covered with the additional concrete shielding (Elwyn and Cossairt 1986).

Spectrum G was obtained on top of the downstream end of a beam dump and target assembly with 800 GeV protons incident on a target followed by bending magnets and a beam absorber. The entire assembly was shielded by an inner layer of iron and an outer layer of concrete comprised of large blocks (0.91 m x 0.91 m x several meters) shown here as for simplicity as monolithic.

Spectrum H was obtained inside a beam enclosure upstream of a target station in which 800 GeV protons struck a beryllium target in an iron cave. The spheres thus measured "backscatter" from this target assembly. Due to the very high radiation levels present, this is the lone spectrum in this set where ^{6}LiF-^{7}LiF thermoluminescent dosimeters (TLDs) were used; the active detector method having unacceptable instrumental dead-time.

Spectrum I was obtained in the second "leg" of a personnel labyrinth. The neutrons were produced by 400 GeV protons striking an aluminum target inside of a large pipe beneath the floor of the main enclosure (Cossairt et al. 1985).

In the present work, the nine spectra were re-analyzed. The relative fluence in each energy bin was extracted from the lethargy plots and multiplied by the value of P_E given by Eqns. (3) and (4) to determine the fractional increment of effective dose due to that particular bin normalized to the total E found by summing over the entire spectrum. Since the energy bin spacings are logarithmic, the dosimetric quantities were evaluated at the geometric means of the bin boundaries. Figs. 8, 9, and 10 show the cumulative distributions of E for the nine spectra; the fraction of E due to neutrons below energy of T_n is plotted as a function of T_n. These plots highlight the relative contributions of different spectral regions to E illustrating the diversity of accelerator neutron energy spectra from a dosimetric viewpoint.

It is useful to have an estimate of the average radiation weighting or effective quality factor of such radiation fields. Furthermore, one needs to compare them with the older values in order to evaluate the changes in instrument calibrations, posting requirements, etc. that are warranted. Each spectrum was combined bin-by-bin with the radiation weighting factors specified in ICRP Publications 103 (ICRP 2007) and 60 (ICRP 1990) to determine its absorbed dose-weighted effective quality factor. Denoted $\langle Q_E \rangle_{103}$ and $\langle Q_E \rangle_{60}$, respectively, these are given in Table 6 along with the earlier values reported (Cossairt et. al. 1988) for $\langle Q_H \rangle$. Also provided are R_{103} and R_{60}, the ratios of these average quality factors to those based on H. For no accelerator neutron spectrum did the effective quality factor exceed 10 using the latest ICRP methodology, establishing this as a bounding value for the effective quality factor of these and

similar neutron spectra. Averages and standard deviations over the nine spectra are provided.

The latest ICRP recommendations (ICRP 2007) result, on average, in an increase of 29 $\pm$ 9 % in the effective quality, or radiation weighting, factor; i.e. from 4.8 to 6.1. This average value remains consistent with the nominal value of 5.0 normally used with the Fermilab chipmunk radiation monitors within the error represented by the standard deviation. From this work, this nominal setting continues to be a viable approximation in lieu of a detailed spectrum measurement, given that the vast majority of neutron radiation fields are either inaccessible to personnel (e.g., inside enclosures) or are of "minimal occupancy". Rare circumstances with higher occupancies may warrant detailed measurements and/or a more conservative choice of quality factors. The chipmunks directly measure an approximation to absorbed dose and apply an instrumental quality factor to approximate the dosimetric quantity of interest, heretofore H, now E. For this purpose, the weighting factor to be applied is the correct choice of parameter. For other types of instruments that measure fluence directly, the appropriate value of P_E should be chosen and/or incorporated into the instrument.

CONCLUSIONS

Dose per fluence factors corresponding to the amended 10 CFR Part 835 as well as the latest ICRP recommendations for neutron radiation fields have been collected, systematized, and applied to both the energy spectra of ^{241}Am-Be sources and to a set of typical neutron radiation fields found at a high energy proton accelerator. These results are likely to be applicable to accelerators of all conceivable energies. They can also be applied correctly in calculations to assure efficient shielding designs.

The average quality factor for the ^{241}Am-Be source associated with E for the emitted neutrons is about 52% higher than that associated with H. Since ^{241}Am-Be sources are often used for the calibration of the neutron-sensitive radiation detectors, this new value needs to be incorporated. The revised calibration will affect field measurements made with the instruments.

For a representative set of accelerator neutron fields, the average effective quality factor was found to increase from 4.8 to 6.1, a relatively small amount. Furthermore, for no accelerator neutron spectrum did the effective quality factor exceed 10. The present nominal quality factor setting of field monitoring equipment used at Fermilab, and perhaps elsewhere, does not need to change significantly. However, instrumentation sensitive to fluence should utilize the dose per fluence factor, P_E.

ACKNOWLEDGEMENTS

This work was, to great degree, inspired by discussions with DeVaughn Nelson. The authors acknowledge helpful comments received from readers of the draft manuscript including Kathy Graden, Susan McGimpsey, Vernon Cupps, David Boehnlein, and Dennis Parzyck.

FOOTNOTES

*Fermi National Accelerator Laboratory, P. O. Box 500, Batavia, IL 60510. Fermilab is operated by Fermi Research Alliance, LLC under Contract No. DE-AC02-07CH11359 with the United States Department of Energy.

For correspondence contact: J. Donald Cossairt at Fermi National Accelerator Laboratory, P. O. Box 500, Batavia, IL 60510, or email at cossairt@fnal.gov.

†With the recent amendments 10 CFR Part 835 continues to require the primary use of the traditional radiological units (rad, rem, etc.), not SI units, for regulatory compliance purposes.

‡The values in Table 1 are equivalent, after unit conversions, to those currently set forth in 10 CFR Part 20 Table 1004(B).2 by the U. S. Nuclear Regulatory Commission for non-DOE, NRC-licensed facilities in the U. S.

§The ICRU sphere, a mathematical construct, has a diameter of 0.3 m, a density of 1.0 g cm^{-3} and a "tissue equivalent" elemental composition of 76.2 % oxygen, 11.1 % carbon, 10.1 % hydrogen, and 2.6 % nitrogen. "Expanded" means the radiation field encompasses the sphere and "aligned" means that the measurement is independent of the angular distribution of the radiation field (Sabol and Weng 1995; Kaye and Laby 2008).

**The use of cm^{-2} as a unit of fluence in the cited references and other publications is nearly universal and will be followed here.

REFERENCES

Awschalom M, Coulson L. A new technique in environmental neutron spectroscopy. In: Synder WS, ed. Proceedings of the 3rd International Congress of the International Radiation Protection Association. Oak Ridge, TN: U.S. Department of Energy Technical Information Center USAEC Conf-730907-P2:1464-1469; 1974.

Bramblett RL, Ewing RI, Bonner TW. A new type of neutron spectrometer. Nucl Instrum and Meth 9:1-12; 1960.

Cossairt JD, Couch JG, Elwyn AJ, Freeman WS. Radiation measurements in a labyrinth penetration at a high-energy proton accelerator. Health Phys 49:907-917; 1985.

Cossairt JD, Elwyn AJ. Personal dosimetry in a mixed field of high-energy muons and neutrons. Health Phys 52:813-818; 1987.

Cossairt JD, Elwyn AJ, Freeman WS, Salsbury WC, Yurista PM. Measurement of neutrons in enclosures and outside of shielding at the Tevatron. In: Proceedings of the 22nd midyear meeting of the Health Physics Society; Topical meeting on instrumentation. San Antonio, TX: 190-199; 1988. Article available from Batavia, IL: Fermi National Accelerator Laboratory Report FERMILAB-Conf-88/106; 1988.

De Guarrina F, Malaroda R. Two different technique measurements of the neutron spectrum of an Am-Be source. Nucl Instrum and Meth 92:277-284; 1971.

Elwyn AJ, Cossairt JD. A study of neutron leakage through an iron shield at an accelerator. Health Phys 51:723-735; 1986.

Ferrari A, Pelliccioni M, Pillon M. Fluence to effective dose conversion coefficients for neutrons up to 10 TeV. Radiat Prot Dosimetry 71:165-173; 1997.

Ferrari A, Pelliccioni M. Fluence to dose equivalent conversion data and effective quality factors for high energy neutrons. Radiat Prot Dosimetry 76:215-224; 1998.

Harvey JR, Mill AJ. A proposed procedure for standardising the relationship between ambient dose equivalent and neutron fluence. Radiat Prot Dosimetry 12:141-143; 1985.

International Commission on Radiological Protection. Recommendations of the International Commission on Radiological Protection. Oxford: Pergamon Press; ICRP Publication 26 Revised; 1981.

International Commission on Radiological Protection. Recommendations of the International Commission on Radiological Protection. Oxford: Pergamon Press; ICRP Publication 60; 1990.

International Commission on Radiological Protection. Dose coefficients for intakes of radionuclides by workers. Oxford: Pergamon Press; ICRP Publication 68; 1994.

International Commission on Radiological Protection. Conversion coefficients for use in radiological protection against external radiation. Oxford: Pergamon Press; ICRP Publication 74; 1996.

International Commission on Radiological Protection. The 2007 recommendations of the International Commission on Radiological Protection. Oxford: Elsevier; ICRP Publication 103; 2007.

International Standards Organization. Reference neutron radiations-Part 1: Characteristics and methods of production. Geneva, Switzerland: International Organization for Standardization; ISO-8529-1; 2001.

Kaye, Laby. Tables of physical constants; section 4.5.4, radiation quantities and units. Institute of Physics, National Physical Laboratory, UK. Available online at

http://www.kayelaby.npl.co.uk/atomic_and_nuclear_physics/4_5/4_5_4.html. (Accessed 14 July 2008.

Krueger F, Larson J. Chipmunk IV: development of and experience with a new generation of radiation monitors for accelerator applications. Nucl Instrum and Meth in Phys Res A495:20-28; 2002.

McCaslin JB, Sun R-K, Swanson WP, Cossairt JD, Elwyn AJ, Freeman WS, Jöstlein H, Moore CD, Yurista PM, Groom DE. Radiation environment in the tunnel of a high-energy proton accelerator at energies near 1 TeV. Presented at the Seventh Annual Congress of the International Radiation Protection Association, Sydney, Australia. April; 1988. Article available from Berkeley, CA: Lawrence Berkeley Laboratory Report LBL-24640; 1988.

National Council on Radiation Protection and Measurements. Protection against neutron radiation. Washington, DC: NCRP Report No. 38; 1971.

Particle Data Group. Review of particle physics. J Phys [G] 33:1-1231; 2006.

Sabol J, Weng P-S. Introduction to radiation protection dosimetry. Singapore: World Scientific; 1995.

Stevenson GR. Dose equivalent per star in hadron cascade calculations. Geneva, Switzerland: European Organization for Nuclear Research Divisional Report TIS-RP/173; 1986.

Sullivan AH, Baarli J. An ionization chamber for the estimation of the biological effectiveness of radiation. Geneva, Switzerland: European Organization for Nuclear Research Report No. 63-17; 1963.

Sutton-Ferenci MR, Hertel NE, Sweezy JE. An evaluated set of neutron, proton and photon fluence-to-effective-dose conversion coefficients. Report DDN #: PPO-P00-G-DDN-X-00008 provided to Los Alamos National Laboratory; 2000. Parts of this work are available elsewhere: Sutton MR, Hertel NE, Waters LS. High-energy neutron dosimetry. J Nucl Sci and Tech, Supplement 1:753-757; (2000); Sutton MR, Hertel NE, Waters LS. Fluence-to-effective-dose conversion coefficients for neutrons up to 2 GeV. In Proceedings of ANS Radiation Protection and Shielding Division Topical Meeting: Radiation protection for our national priorities: medicine, the environment and the legacy, Spokane, WA:176-180; 2001; Sutton MR, Hertel NE, Waters LS. Fluence-to-effective-dose conversion coefficients for high-energy radiations calculated with MCNPX**.** Paris, France: SATIF-5; Shielding of accelerators, testing and irradiation facilities, July 20-21, 2000.

U. S. Department of Energy. Procedural rules for DOE nuclear activities and occupational radiation protection; final rule. Washington, DC: U. S. Government Printing Office; 10 CFR Parts 820 and 835. Federal Register 72:31904-31941; 8 June 2007.

U. S. Department of Energy. Radiation protection of the public and the environment. Washington, DC: DOE Order 5400.5, Change 2; 7 January 1993.

Veinot KG, Hertel NE. Effective quality factors for neutrons based on the revised ICRP/ICRU recommendations. Radiat Prot Dosimetry 115:536-641; 2005.

Zimbal A. Measurement of the spectral fluence rate of reference neutron sources with a liquid scintillation detector. Radiat Prot Dosimetry 126: 413-417; 2007.

TABLES

Table 1. Values of the quality factor, Q_H, and the dose equivalent per fluence, $P_H = H\,\Phi^{-1}$, found in pre-2007 versions of 10 CFR Part 835 as adapted from NCRP Report 38 (NCRP 1971) for specific neutron kinetic energies, T_n.

T_n (MeV)	Q_H	P_H (pSv cm^2)
2.5 x 10^{-8}	2	10.2
1 x 10^{-7}	2	10.2
1 x 10^{-6}	2	12.4
1 x 10^{-5}	2	12.4
1 x 10^{-4}	2	12.0
1 x 10^{-3}	2	10.2
1 x 10^{-2}	2.5	9.9
0.1	7.5	60.4
0.5	11	257.2
1	11	365.5
2.5	9	347.2
5	8	434.0
7	7	408.5
10	6.5	408.5
14	7.5	578.7
20	8	631.3
40	7	694.4
60	5.5	631.3
100	4	496.0
200	3.5	534.2
300	3.5	631.3
400	3.5	694.4

Table 2 Curve fitting constants used to fit P_E.

Parameters for Eq. (3)	Values
a	0.952848
b	-1.12792
c	-0.236271
d	2.42754
f	-1.02834
g	1.38158
h	0.702555
j	13.9688
k	4.91135
Parameters for Eq. (4)	Values
m	98.4299
p	0.368465

Table 3 Values P_E calculated using Eqns. (3) and (4) as a function of neutron kinetic energy, T_n.

T_n (MeV)	P_E (pSv cm^2)	T_n (MeV)	P_E (pSv cm^2)	T_n (MeV)	P_E (pSv cm^2)
1.0×10^{-9}	3.00	0.20	55.8	30	417
1.0×10^{-8}	4.01	0.30	74.5	40	426
2.5×10^{-8}	4.56	0.50	106	50	432
1.0×10^{-7}	5.58	0.70	131	60	436
2.0×10^{-7}	6.17	0.90	152	75	441
5.0×10^{-7}	6.99	1.0	161	100	449
1.0×10^{-6}	7.60	1.2	178	130	459
2.0×10^{-6}	8.16	1.5	199	150	466
5.0×10^{-6}	8.76	2.0	226	180	479
1.0×10^{-5}	9.06	2.5	248	200	488
2.0×10^{-5}	9.18	3.0	265	300	551
5.0×10^{-5}	9.10	4.0	292	400	637
1.0×10^{-4}	8.89	5.0	311	500	740
2.0×10^{-4}	8.62	6.0	326	700	971
5.0×10^{-4}	8.30	7.0	338	1.0×10^{3}	1290
1.0×10^{-3}	8.19	8.0	348	1.5×10^{3}	1640
2.0×10^{-3}	8.34	9.0	357	2.0×10^{3}	1820
5.0×10^{-3}	9.19	10	364	3.0×10^{3}	1960
1.0×10^{-2}	10.7	12	375	5.0×10^{3}	2270
2.0×10^{-2}	13.7	14	384	1.0×10^{4}	2930
3.0×10^{-2}	16.5	15	387	2.0×10^{4}	3780
5.0×10^{-2}	21.8	16	391	5.0×10^{4}	5300
7.0×10^{-2}	26.8	17	394	1.0×10^{5}	6850
0.10	34.1	18	396	1.0×10^{6}	16000
0.15	45.3	20	401	1.0×10^{7}	37400

Table 4 Values w_R calculated using Eqns. (5) through (8) as a function of neutron kinetic energy, T_n.

T_n (MeV)	$w_{R,60}$	$w_{R,103}$	T_n (MeV)	$w_{R,60}$	$w_{R,103}$	T_n (MeV)	$w_{R,60}$	$w_{R,103}$
1.0×10^{-9}	5.00	2.50	0.20	19.8	14.3	30	6.04	6.04
1.0×10^{-8}	5.00	2.50	0.30	21.3	16.8	40	5.69	5.69
2.5×10^{-8}	5.00	2.50	0.50	22.0	19.3	50	5.50	5.50
1.0×10^{-7}	5.00	2.50	0.70	21.7	20.3	60	5.37	5.36
2.0×10^{-7}	5.00	2.50	0.90	21.0	20.7	75	5.26	5.16
5.0×10^{-7}	5.00	2.50	1.0	20.7	20.7	100	5.16	4.86
1.0×10^{-6}	5.00	2.50	1.2	20.0	20.0	130	5.10	4.57
2.0×10^{-6}	5.00	2.50	1.5	18.9	18.9	150	5.08	4.40
5.0×10^{-6}	5.00	2.50	2.0	17.3	17.3	180	5.05	4.20
1.0×10^{-5}	5.00	2.50	2.5	16.0	16.0	200	5.04	4.08
2.0×10^{-5}	5.00	2.50	3.0	15.0	15.0	300	5.02	3.66
5.0×10^{-5}	5.00	2.50	4.0	13.3	13.3	400	5.01	3.40
1.0×10^{-4}	5.00	2.50	5.0	12.0	12.0	500	5.00	3.23
2.0×10^{-4}	5.00	2.50	6.0	11.1	11.1	700	5.00	3.01
5.0×10^{-4}	5.01	2.50	7.0	10.3	10.3	1.0×10^{3}	5.00	2.84
1.0×10^{-3}	5.03	2.51	8.0	9.72	9.72	1.5×10^{3}	5.00	2.70
2.0×10^{-3}	5.11	2.53	9.0	9.22	9.22	2.0×10^{3}	5.00	2.63
5.0×10^{-3}	5.50	2.67	10	8.81	8.81	3.0×10^{3}	5.00	2.57
1.0×10^{-2}	6.33	3.03	12	8.16	8.16	5.0×10^{3}	5.00	2.53
2.0×10^{-2}	8.02	3.92	14	7.67	7.67	1.0×10^{4}	5.00	2.51
3.0×10^{-2}	9.55	4.84	15	7.47	7.47	2.0×10^{4}	5.00	2.50
5.0×10^{-2}	12.0	6.58	16	7.30	7.30	5.0×10^{4}	5.00	2.50
7.0×10^{-2}	13.9	8.10	17	7.14	7.14	1.0×10^{5}	5.00	2.50
0.10	16.0	10.0	18	7.00	7.00	1.0×10^{6}	5.00	2.50
0.15	18.4	12.5	20	6.76	6.76	1.0×10^{7}	5.00	2.50

Table 5 Computed properties of reference ^{241}Am-Be neutron energy spectra.

Parameter	ISO 8259-1 Spectrum	DeGuarrini and Malaroda Spectrum
$\langle T_n \rangle$ (MeV)	4.17	3.98
$\langle Q_E \rangle_{60}$	12.4	12.8
$\langle Q_E \rangle_{103}$	12.4	12.7
$\langle Q_H \rangle$	8.17	8.35
$\langle Q_E \rangle_{103}/\langle Q_H \rangle$	1.52	1.52
$\langle P_E \rangle_{103}$ (pSv cm^2)	268	265
$\langle P_H \rangle$ (pSv cm^2)	376	380
$\langle P_E \rangle_{103}/\langle P_H \rangle$	0.713	0.697

Table 6 Quality factors of Fermilab neutron energy spectra shown in Figs. 5 through 7.

Spectrum	$\langle Q_H \rangle$[a]	ICRP 103 Results		ICRP 60 Results	
		$\langle Q_E \rangle_{103}$	R_{103}	$\langle Q_E \rangle_{60}$	R_{60}
A: Debuncher Ring	5.8	7.54	1.30	7.74	1.33
B: Debuncher Ring with Fe	4.2	4.71	1.12	5.32	1.27
C: Tevatron Tunnel	6.9	9.46	1.42	11.4	1.64
D: P-Center Roof	6.2	8.15	1.32	9.50	1.53
E: M-East "Before"	5.4	6.61	1.23	8.23	1.52
F: M-East "After"	2.5	3.64	1.46	6.45	2.58
G: M-Center	3.4	4.27	1.26	5.96	1.75
H: M-West Interior	5.7	6.55	1.15	8.72	1.53
I: N-West Labyrinth	3.1	4.25	1.37	6.13	1.98
Average Values	4.8	6.13	1.29	7.72	1.68
Standard Deviation (%)	32	33	8.9	26	24

[a]As determined by Cossairt et al. (1988).

List of Figure Captions

1. Values for dose per fluence factors discussed in the text as a function of neutron kinetic energy T_n. Those for P_H (1971) are from NCRP Report 38 (1971). Those for P_E (ROT) (S-F, 2000) are from Sutton-Ferenci, et al. (2000) for ROT geometry including both tabulations (data points) and Eq. (3) (solid line). Those for P_E (ISO) (F, 1997) are from Ferrari, et al. (1997) for ISO geometry. Those for P^* (S, 1986) are from Stevenson (1986). Those for P_E (ROT, 1996) for ROT geometry are from ICRP Publication 74 (ICRP 1996). Those for P_p (V, 2005) and for P^* (V, 2005), respectively, are from Veinot and Hertel (2005). The power law fit to the high energy values [Eq. (4)] of P_E (ISO) (F 1997) is also shown.

2. Values of radiation weighting and quality factors used in the model of Eq. (1) to connect absorbed dose with other dosimetric quantities. ICRP 60 w_R, ICRP 74 Q_E, ICRP 103 w_R , and NCRP 38 Q_H are values provided in ICRP Publications 60 (ICRP 1990), 74 (ICRP 1996), 103 (ICRP 2007), and NCRP Report 38 (NCRP 1971), respectively. The quality factors Q_p (V, 2005), and Q^* (V, 2005) obtained by Veinot and Hertel (2005) as well as Q_E (F, 1998) calculated by Ferrari et al. (1998) are also shown.

3. Energy spectrum of neutrons emitted by ^{241}Am-Be neutron sources. The ISO 8529-1 spectrum (ISO 2001) adapted from Zimbal (2007) is shown along with that adapted from DeGuarrini and Malaroda (1979).

4. Fractions of effective dose, E, absorbed dose, D, and dose equivalent, H, due to neutrons with kinetic energy $T < T_n$ as a function of T_n for the ISO 8529-1 ^{241}Am-Be neutron energy spectrum. The values of D were deduced using the weighting factors w_R of ICRP Publication 103. The values of H were calculated by linear interpolation between the values of Table 1. The quantities plotted are limited to neutrons only, excluding any contributions from any other radiations (e.g., photons) present.

5. Shielding geometries (left) and corresponding unfolded neutron energy spectra (right) for spectra A, B, and C. The ordinates of the graphs are in arbitrary units of neutrons per logarithmic energy interval (Cossairt et al. 1988).

6. Shielding geometries (left) and corresponding unfolded neutron energy spectra (right) for spectra D, E, and F. Spectrum E was measured before the addition of the cross-hatched concrete blocks while spectrum F was measured after the addition of those blocks. The ordinates of the graphs are in arbitrary units of neutrons per logarithmic energy interval (Cossairt et al. 1988).

7. Shielding geometries (left) and corresponding unfolded neutron energy spectra (right) for spectra G, H, and I. The ordinates of the graphs are in arbitrary units of neutrons per logarithmic energy interval (Cossairt et al. 1988).

8. Fractions of effective dose, E, due to neutrons with kinetic energy $T < T_n$ as a function of T_n for spectra A, B, and C.

9. Fractions of effective dose, E, due to neutrons with kinetic energy $T < T_n$ as a function of T_n for spectra D, E, and F.

10. Fractions of effective dose, E, due to neutrons with kinetic energy $T < T_n$ as a function of T_n for spectra G, H, and I.

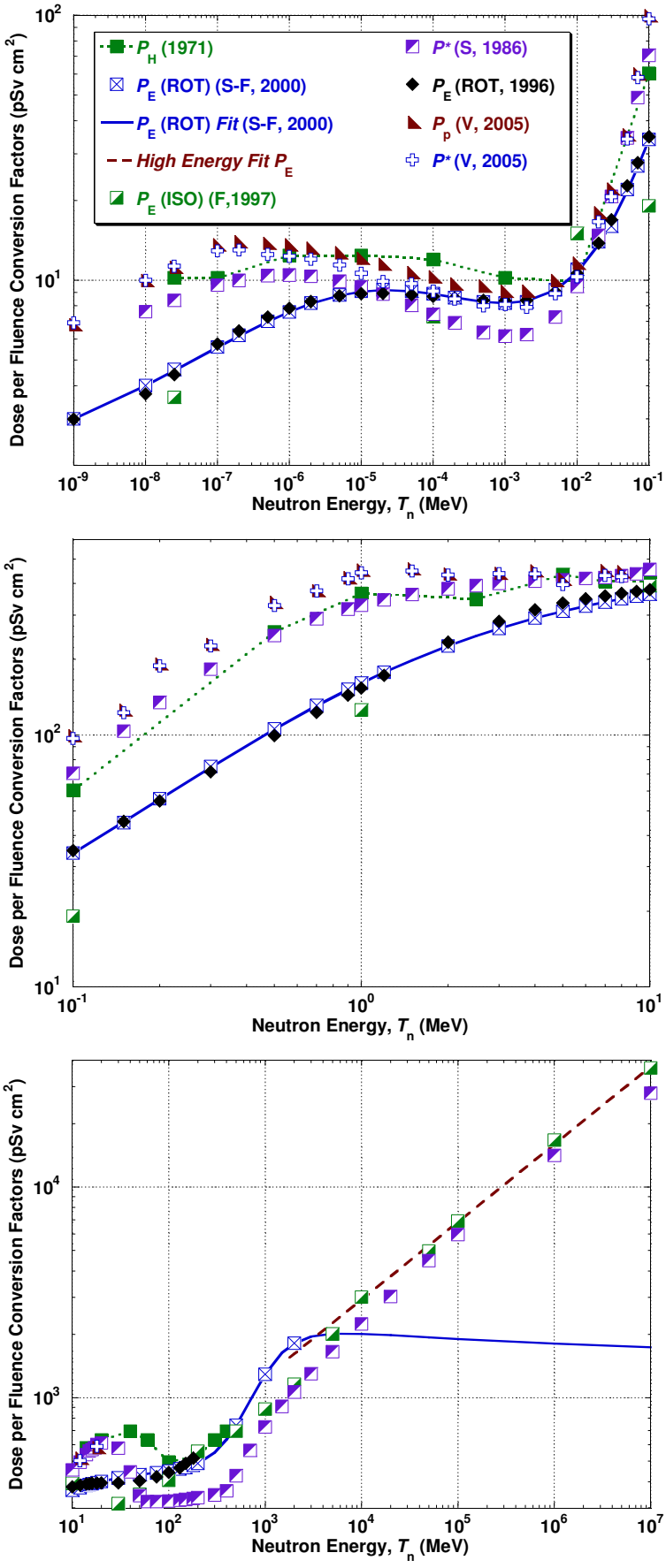
P_H (1971)
P_E (ROT) (S-F, 2000)
P_E (ROT) *Fit* (S-F, 2000)
High Energy Fit P_E
P_E (ISO) (F,1997)
P^* (S, 1986)
P_E (ROT, 1996)
P_p (V, 2005)
P^* (V, 2005)
Dose per Fluence Conversion Factors (pSv cm^2)
Neutron Energy, T_n (MeV)

Fig. 1

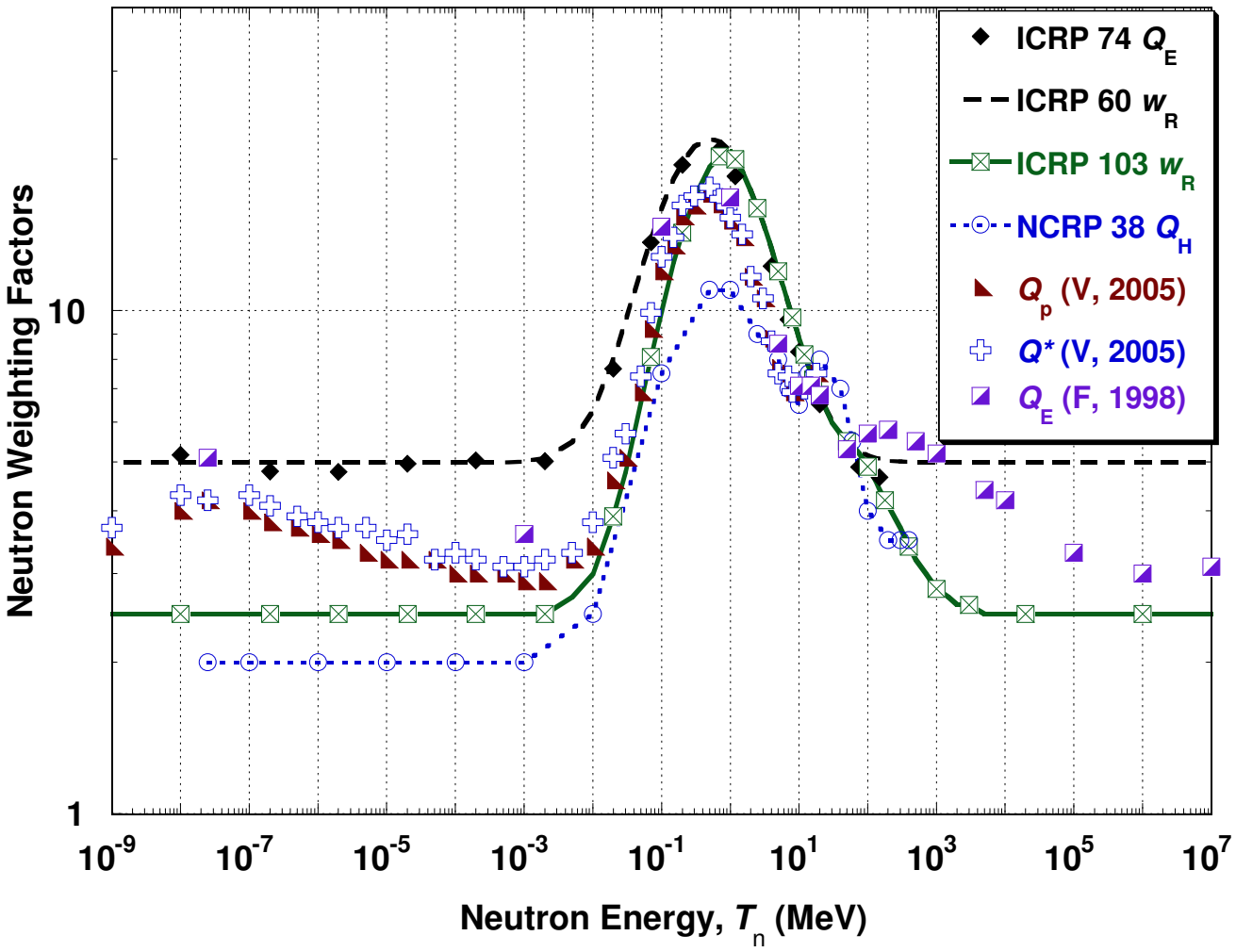
ICRP 74 Q_E
ICRP 60 w_R
ICRP 103 w_R
NCRP 38 Q_H
Q_p (V, 2005)
Q^* (V, 2005)
Q_E (F, 1998)
Neutron Weighting Factors
10
1
10^{-9}
10^{-7}
10^{-5}
10^{-3}
10^{-1}
10^{1}
10^{3}
10^{5}
10^{7}
Neutron Energy, T_n (MeV)

Fig. 2

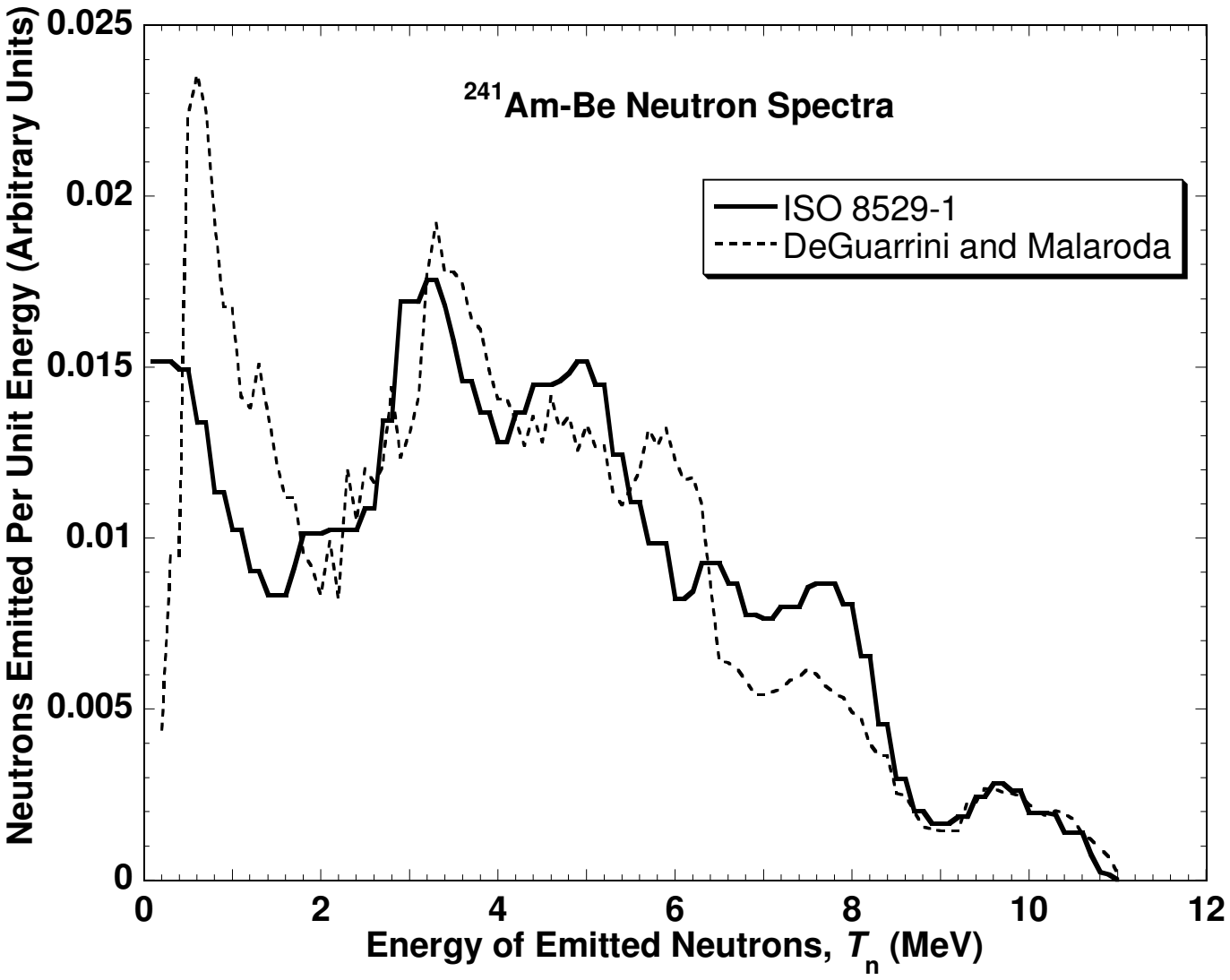
241Am-Be Neutron Spectra
ISO 8529-1
DeGuarrini and Malaroda
Neutrons Emitted Per Unit Energy (Arbitrary Units)
0.025
0.02
0.015
0.01
0.005
0
0
2
4
6
8
10
12
Energy of Emitted Neutrons, T_n (MeV)

Fig. 3

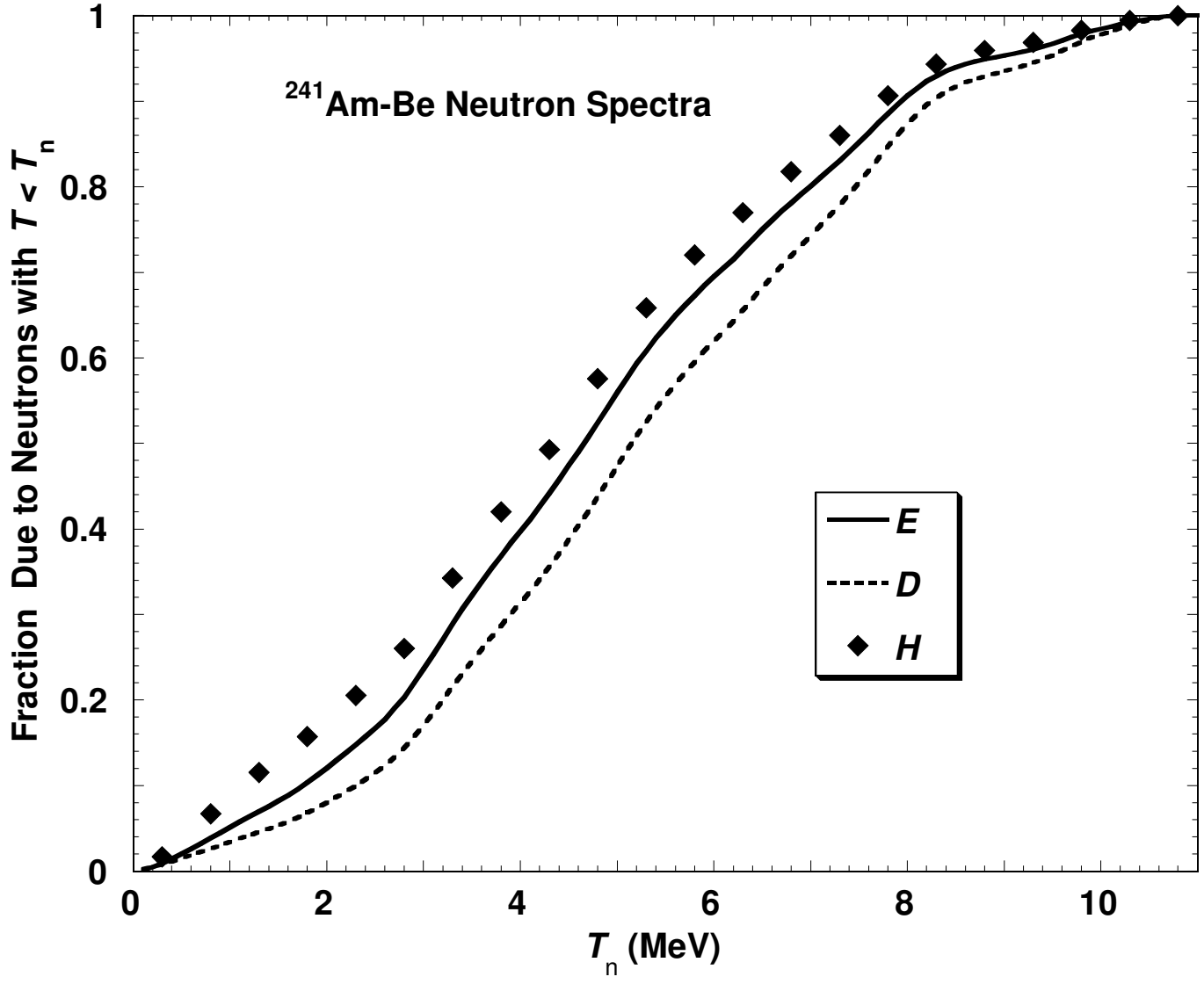
241Am-Be Neutron Spectra
Fraction Due to Neutrons with T < Tn
Tn (MeV)
E
D
H
0
0.2
0.4
0.6
0.8
1
0
2
4
6
8
10

Fig. 4

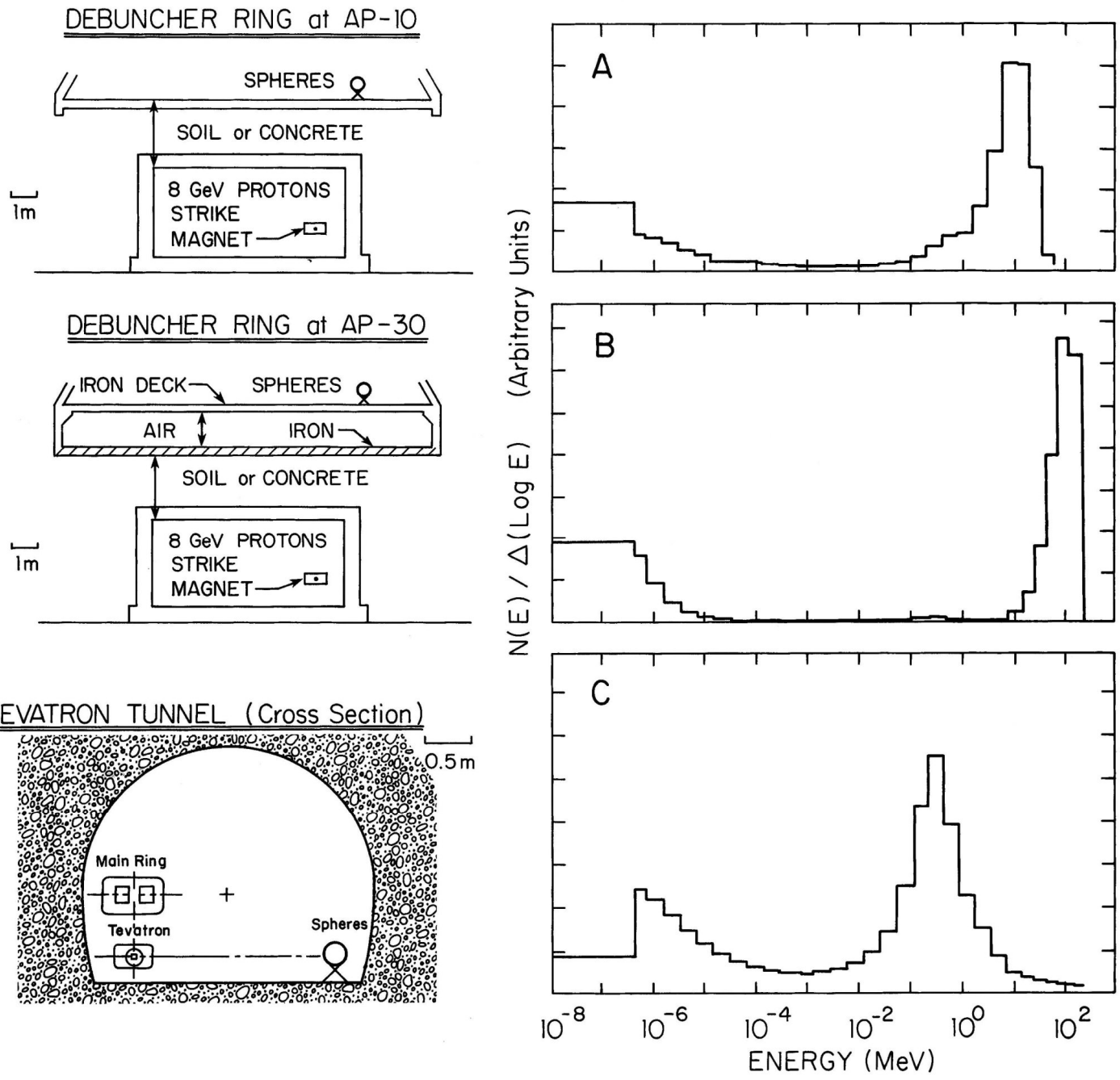
DEBUNCHER RING at AP-10
SPHERES
SOIL or CONCRETE
8 GeV PROTONS
STRIKE
MAGNET
1m
DEBUNCHER RING at AP-30
IRON DECK
SPHERES
AIR
IRON
SOIL or CONCRETE
8 GeV PROTONS
STRIKE
MAGNET
1m
TEVATRON TUNNEL (Cross Section)
0.5m
Main Ring
Tevatron
Spheres
A
B
C
N(E) / Δ(Log E) (Arbitrary Units)
10^-8
10^-6
10^-4
10^-2
10^0
10^2
ENERGY (MeV)

Fig. 5

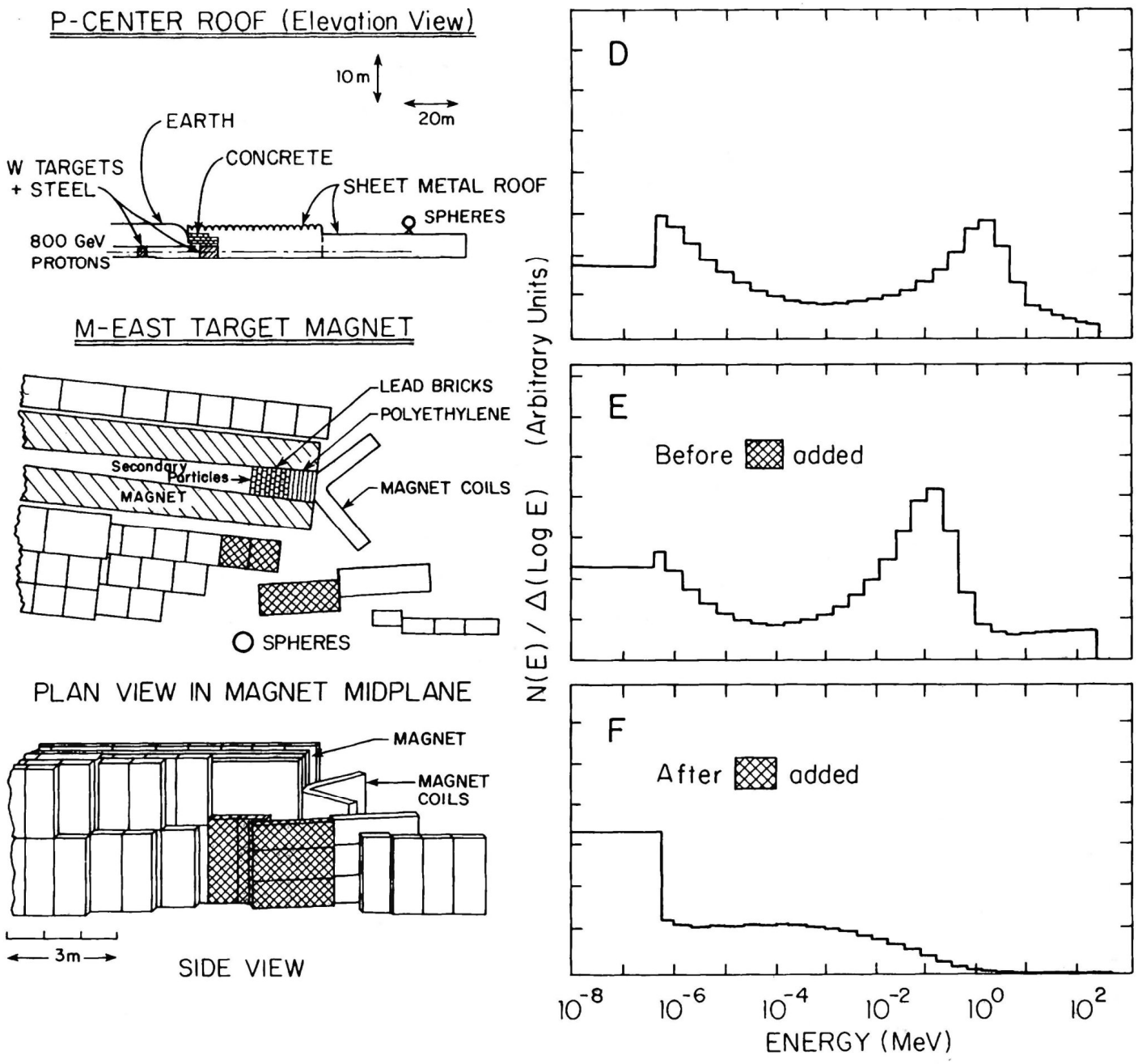
P-CENTER ROOF (Elevation View)
10m
20m
EARTH
CONCRETE
W TARGETS
+ STEEL
SHEET METAL ROOF
SPHERES
800 GeV
PROTONS
M-EAST TARGET MAGNET
LEAD BRICKS
POLYETHYLENE
Secondary
Particles
MAGNET
MAGNET COILS
SPHERES
PLAN VIEW IN MAGNET MIDPLANE
MAGNET
MAGNET
COILS
3m
SIDE VIEW
D
E
Before added
F
After added
N(E) / Δ(Log E) (Arbitrary Units)
10^-8
10^-6
10^-4
10^-2
10^0
10^2
ENERGY (MeV)

Fig. 6

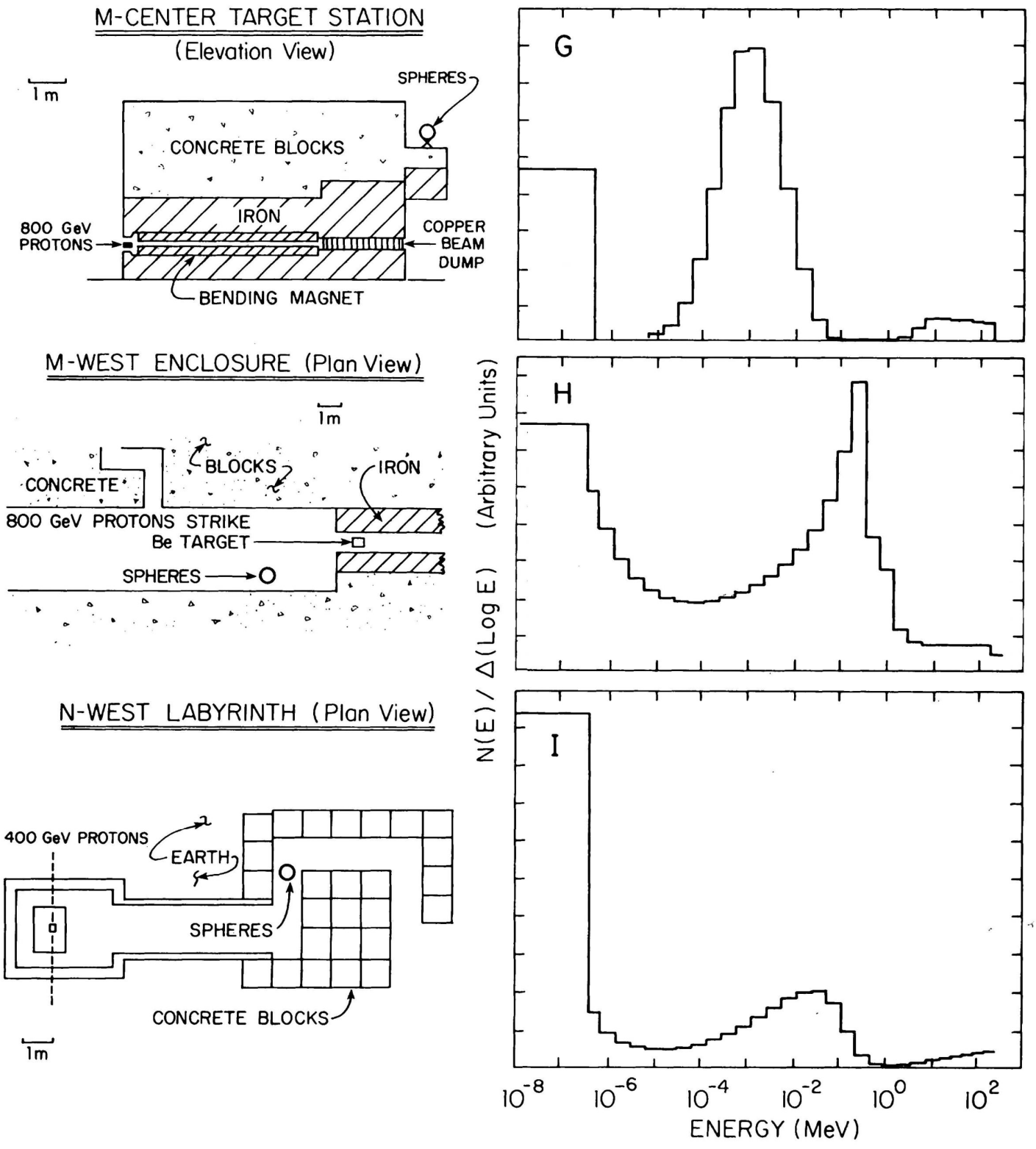
M-CENTER TARGET STATION
(Elevation View)
1 m
SPHERES
CONCRETE BLOCKS
IRON
800 GeV
PROTONS
COPPER
BEAM
DUMP
BENDING MAGNET
M-WEST ENCLOSURE (Plan View)
1m
CONCRETE
BLOCKS
IRON
800 GeV PROTONS STRIKE
Be TARGET
SPHERES
N-WEST LABYRINTH (Plan View)
400 GeV PROTONS
EARTH
SPHERES
CONCRETE BLOCKS
1m
G
H
I
N(E) / Δ(Log E) (Arbitrary Units)
10^-8
10^-6
10^-4
10^-2
10^0
10^2
ENERGY (MeV)

Fig. 7

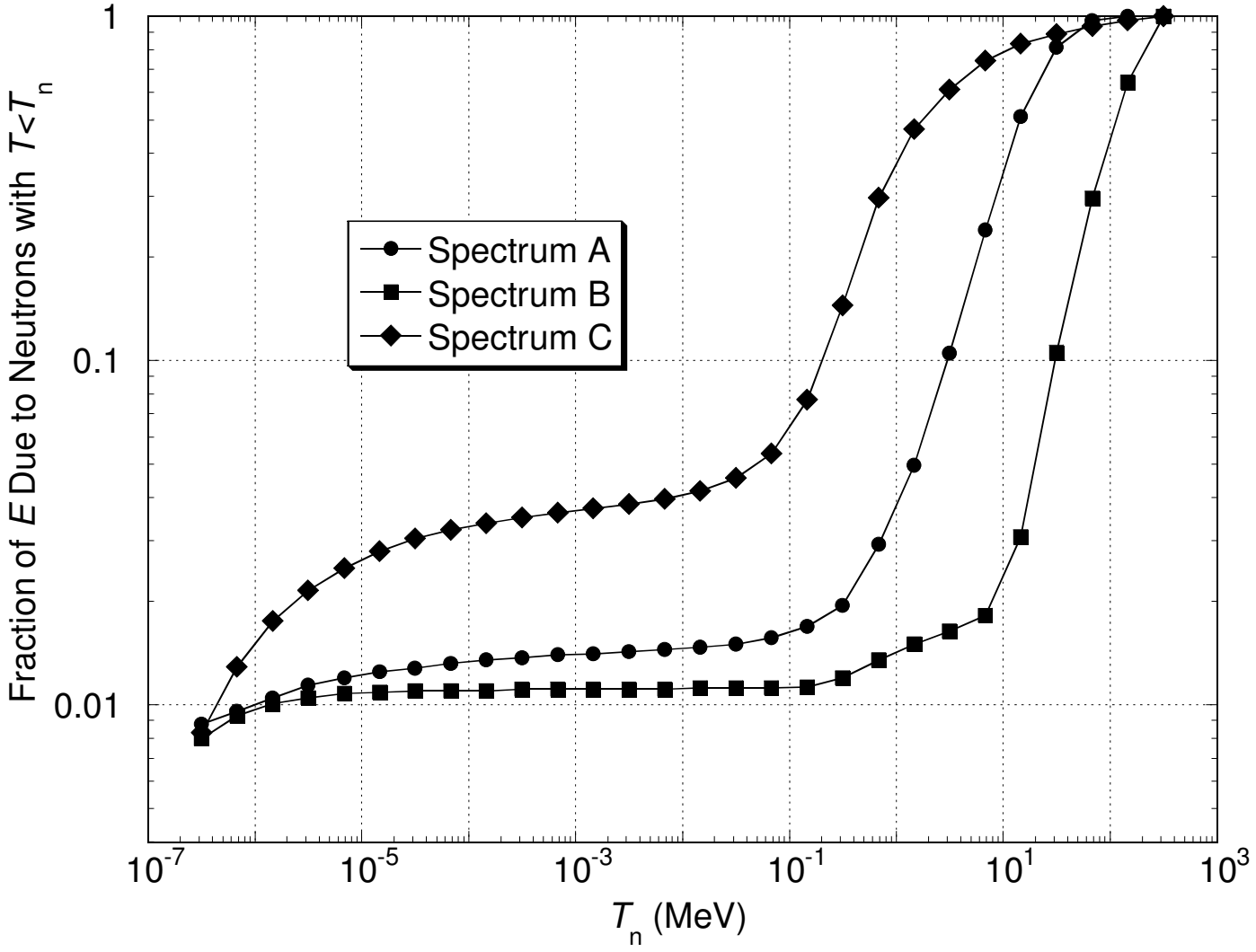
Fraction of E Due to Neutrons with $T<T_n$
1
0.1
0.01
10^{-7}
10^{-5}
10^{-3}
10^{-1}
10^{1}
10^{3}
T_n (MeV)
Spectrum A
Spectrum B
Spectrum C

Fig. 8

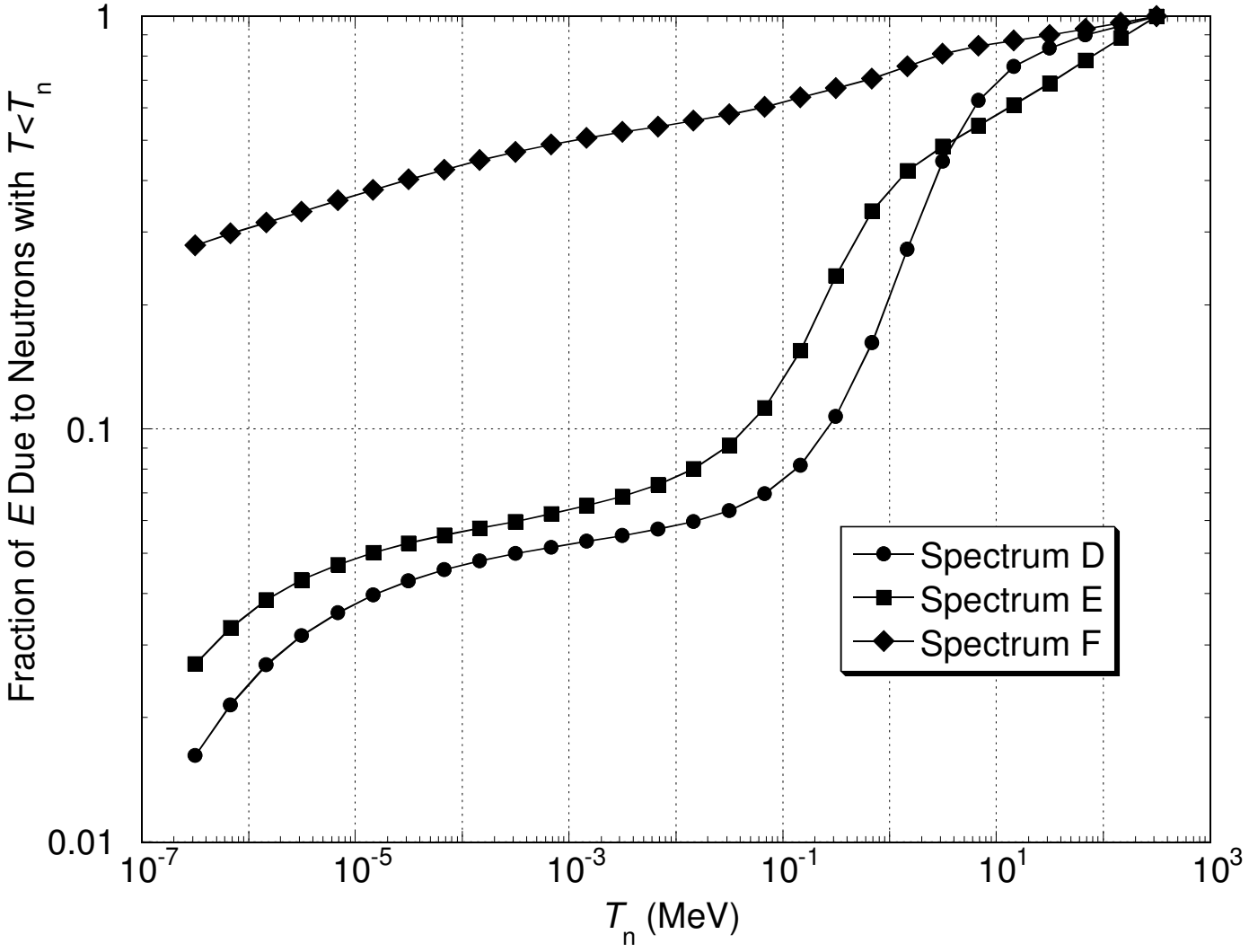
1
0.1
0.01
Fraction of E Due to Neutrons with T<T_n
10^-7
10^-5
10^-3
10^-1
10^1
10^3
T_n (MeV)
Spectrum D
Spectrum E
Spectrum F

Fig. 9

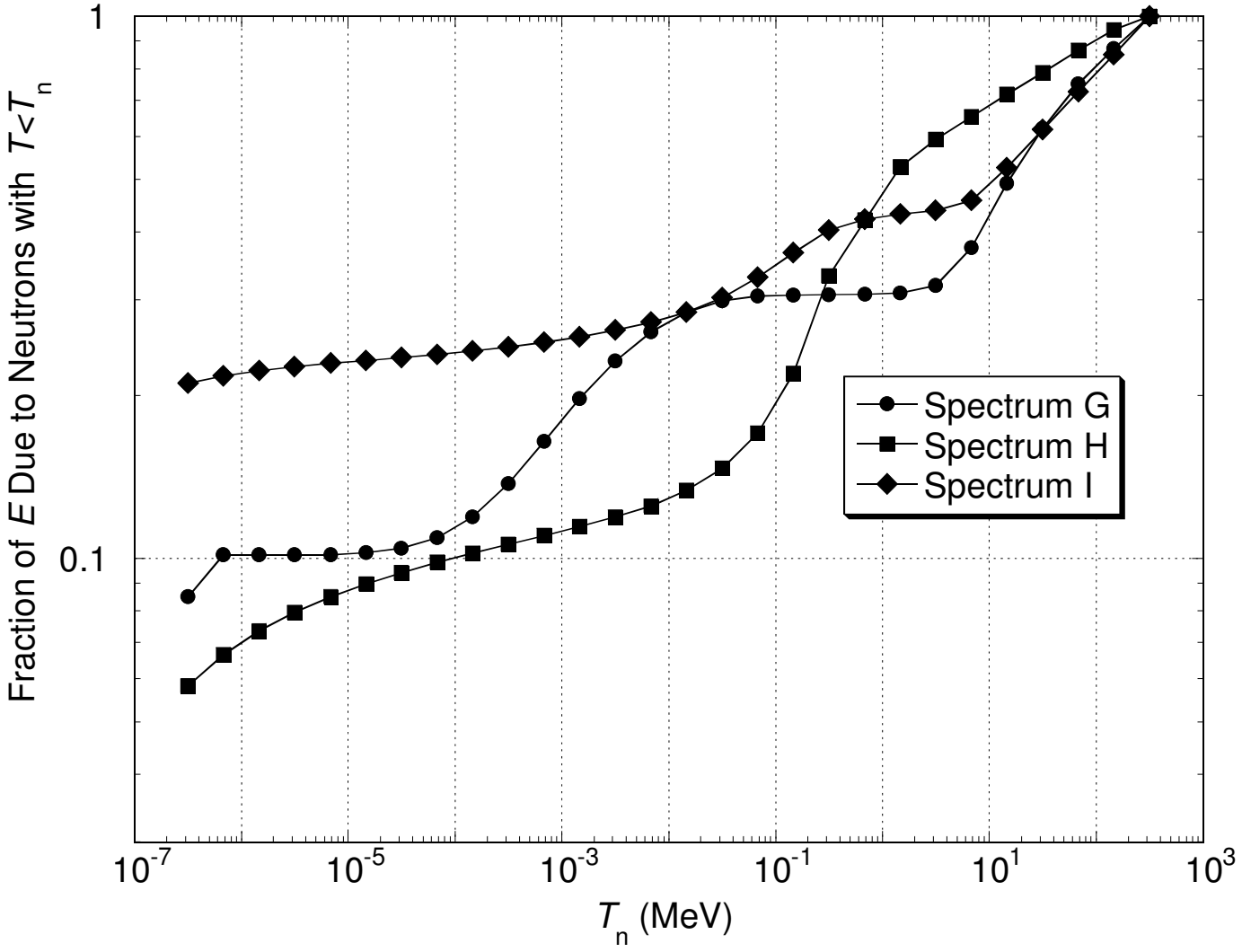
1
0.1
Fraction of E Due to Neutrons with T<T_n
10^-7
10^-5
10^-3
10^-1
10^1
10^3
T_n (MeV)
Spectrum G
Spectrum H
Spectrum I

Fig. 10